

Aortoiliac hemodynamic and morphologic adaptation to chronic spinal cord injury

Janice J. Yeung, MD,^{a,b} Hyun Jin Kim, MS,^c Thomas A. Abbruzzese, MD,^b Irene E. Vignon-Clementel, PhD,^c Mary T. Draney-Blomme, PhD,^c Kay K. Yeung, MD,^b Inder Perakash, MD,^d Robert J. Herfkens, MD,^c Charles A. Taylor, PhD,^{b,f} and Ronald L. Dalman, MD, FACS,^b *Stanford, Calif; and Rochester, NY*

Background: Reduced lower limb blood flow and resistive hemodynamic conditions potentially promote aortic inflammation and aneurysmal degeneration. We used abdominal ultrasonography, magnetic resonance imaging, and computational flow modeling to determine the relationship between reduced infrarenal aortic blood flow in chronic spinal cord injury (SCI) subjects and risk for abdominal aortic aneurysm (AAA) disease.

Methods: Aortic diameter in consecutive SCI subjects (n = 123) was determined via transabdominal ultrasonography. Aortic anatomic and physiologic data were acquired via magnetic resonance angiography (MRA; n = 5) and cine phase-contrast magnetic resonance flow imaging (n = 4) from SCI subjects whose aortic diameter was less than 3.0 cm by ultrasonography. Computational flow models were constructed from magnetic resonance data sets. Results were compared with those obtained from ambulatory control subjects (ultrasonography, n = 129; MRA/phase-contrast magnetic resonance flow imaging, n = 6) who were recruited at random from a larger pool of risk factor-matched individuals without known AAA disease.

Results: Age, sex distribution, and smoking histories were comparable between the SCI and control groups. In the SCI group, time since injury averaged 26 ± 13 years (mean ± SD). Aortic diameter was larger (P < .01), and the prevalence of large (≥2.5 cm; P < .01) or aneurysmal (≥3.0 cm; P < .05) aortas was greater in SCI subjects. Paradoxically, common iliac artery diameters were reduced in SCI subjects (<1.0 cm; 48% SCI vs 26% control; P < .0001). Focal preaneurysmal enlargement was noted in four of five SCI subjects by MRA. Flow modeling revealed normal flow volume, biphasic and reduced oscillatory flow, slower pressure decay, and reduced wall shear stress in the SCI infrarenal aorta.

Conclusions: Characteristic aortoiliac hemodynamic and morphologic adaptations occur in response to chronic SCI. Slower aortic pressure decay and reduced wall shear stress after SCI may contribute to mural degeneration, enlargement, and an increased prevalence of AAA disease. (J Vasc Surg 2006;44:1254-65.)

Aortic diameter increases normally as a function of age. When diameter equals or exceeds 3 cm, however, the abdominal aorta is considered aneurysmal.¹⁻³ Pathologic enlargement occurs most commonly in the distal aorta, the region caudal to the renal arteries. Compared with more proximal segments, the resting infrarenal aortic hemodynamic environment is characterized by increased peripheral resistance, increased oscillatory wall shear stress (WSS), and

reduced flow.⁴ These “resistive” hemodynamic conditions may predispose the infrarenal aorta to occlusive or aneurysmal degeneration. Major limb amputation,⁵ hemiparesis,⁶ chronic spinal cord injury (SCI),⁷ and severe peripheral vascular disease⁸ have recently been recognized as potential independent risk factors for infrarenal aortic disease, associations that highlight the potential pathogenic significance of resistive hemodynamic conditions.

In our surgical practice, we noted that aortic aneurysm disease or a history of abdominal aortic aneurysm (AAA) repair seemed unusually prevalent among chronic SCI patients. Among other risk factors for vascular diseases present in SCI patients,⁹⁻¹³ permanent reduction in infrarenal aortic blood flow due to denervated and immobile lower extremities may also promote aortic degeneration. We used magnetic resonance imaging (MRI) and computational fluid dynamics to analyze the influence of resistive hemodynamic conditions on AAA pathogenesis in SCI subjects and risk factor-matched ambulatory control subjects.

METHODS

All protocols were designed in accordance with Good Clinical Practice guidelines for human research and were approved by the Institutional Review Board of Stanford University and the Veterans Affairs Palo Alto Health Care System (VAPAHCS). Informed consent was obtained be-

From the Department of Surgery, University of Rochester,^a Department of Surgery, Division of Vascular Surgery,^b Department of Mechanical Engineering,^c Department of Radiology,^c and Department of Bioengineering,^f Stanford University, and the Palo Alto Spinal Cord Injury Unit, Palo Alto Veterans Affairs Health Care System.^d

Supported by the Paralyzed Veterans of America, the Palo Alto Institute for Research and Education, the Lifeline Foundation, the National Science Foundation (Grant 0205741), the National Heart, Lung and Blood Institute (R01 HL064338-05A2), the Lucas Foundation, GE Medical Systems, the American Heart Association, Alpha Omega Alpha Honor Medical Society, and the University of Wisconsin Cardiovascular Research Center.

Competition of interest: none.

Presented at the Twentieth Annual Meeting of the Western Vascular Society, Park City, Utah, Sept. 24-27, 2005.

Additional material for this article may be found online at www.jvascsurg.org.

Reprint requests: Ronald L. Dalman, MD, FACS, Vascular Center, Suite H3542, Stanford University Medical Center, 300 Pasteur Dr, Stanford, CA 94305 (e-mail: rld@stanford.edu).

0741-5214/\$32.00

Copyright © 2006 by The Society for Vascular Surgery.

doi:10.1016/j.jvs.2006.08.026

fore participation. No monetary compensation was provided for study participation.

Study groups. SCI subjects were recruited from consecutive VAPAHCS patients presenting for annual health maintenance examinations between January 1, 1999, and August 6, 2004. Subjects participated by completing a questionnaire and undergoing a fasting abdominal ultrasound AAA screening examination ($n = 121$) or alternative abdominal imaging studies ($n = 2$). Five SCI subjects also underwent secondary magnetic resonance angiography (MRA).

Control subjects were identified from a Health Insurance Portability and Accountability Act-compliant database composed of non-SCI VAPAHCS patients selected for demographic (eg, sex and age) and social (eg, smoking status) similarity to the overall SCI cohort. Potential subjects identified at random from this database were contacted by mail and a follow-up telephone call regarding study participation. Five hundred nineteen subjects were contacted, and 129 subjects were enrolled. Six subjects in this group also underwent MRA examinations.

Inclusion criteria for both SCI and control subject participation included age greater than 50 years without a prior diagnosis of AAA disease or history of aortic or iliac surgery. SCI subjects were eligible for participation only if 5 years or more had elapsed since injury. SCI and control subjects were queried regarding biomorphic indices and the presence of known risk factors for peripheral vascular and aortic disease. SCI subjects were also queried regarding the nature and history of their injury.

Aortic and iliac artery imaging. Each subject underwent fasting abdominal ultrasound imaging limited to the aorta and iliac arteries. All studies were performed by a registered vascular technologist by using either an Acuson Sequoia (Siemens Medical Solutions, Malvern, Pa) or ATL Philips Medical HDI 5000 machine (Royal Philips Electronics, The Netherlands) equipped with 3.5-MHz transducers. Maximal aortic diameter was determined from anteroposterior and lateral measurements obtained between the renal arteries and aortic bifurcation. When sufficiently well visualized, the maximum anteroposterior and lateral diameters of the common iliac arteries were also recorded. Heart rate, systolic and diastolic blood pressures, and femoral pulse status (present or absent) on physical examination were also recorded. For two SCI subjects, measurements were obtained from vascular contrast-enhanced computed tomographic images ordered for unrelated clinical conditions.

Clinical data analysis. Aortas with a diameter of 3.0 cm or more were classified as aneurysmal. Aortas with diameters of 2.5 cm or more were considered to be enlarged; this group also included subjects with AAA (≥ 3.0 cm). Aortic diameter less than 2.5 cm was considered normal. There was no category for smaller or hypoplastic aortas. Iliac artery diameter measurements were divided into aneurysmal (≥ 1.5 cm), enlarged (≥ 1.25 cm, includes aneurysms), and very small (< 1.0 cm) groups. Before the initiation of the study, a sample size of 125 subjects in each group was projected to provide sufficient power ($\beta = .80$)

to detect a difference of 12% in AAA prevalence between SCI and control subjects. Significance was determined at the .05 level. Continuous data were analyzed by using t tests. Two-tailed P values were calculated for all parameters except iliac and aortic diameter comparisons between groups. Categorical data were analyzed with a two-tailed Fisher exact test.

MRA and imaging. Five SCI and six control subjects underwent additional imaging via magnetic resonance arteriography. Potential angiography MRA subjects were selected randomly from those determined to be free from aortic or iliac aneurysms at the initial ultrasound study or contraindications to MRI. All imaging was performed at Stanford University's Richard M. Lucas Center for Magnetic Resonance Spectroscopy and Imaging by using a 1.5-T GE Signa (GE Medical Systems, Milwaukee, Wis) magnetic resonance scanner. A three-dimensional fast gradient-recalled sequence was performed after intravenous administration of 0.2 mmol/kg of gadolinium-based contrast material, injected at a rate of 2 to 3 mL/s starting approximately 15 seconds before the MRA scan. Scan parameters included a repetition time of 13.9 milliseconds, an echo time of 2.8 milliseconds, and a flip angle of 40°. The previous steps were repeated as needed to acquire a second three-dimensional contrast-enhanced volumetric scan partially overlapping the original three-dimensional acquisition, to span the required anatomic range and minimize uncorrected distortions.

Phase-contrast MRI (PC-MRI) techniques were subsequently applied to acquire time-resolved anatomic data and through-plane blood flow velocity maps perpendicular to the aorta at the supraceliac and infrarenal levels. Acquisitions were gated to the cardiac cycle with a 4-lead electrocardiograph monitor, and image data were retrospectively reconstructed to 24 evenly spaced time points over the cardiac cycle and corrected with a first-order baseline correction method. Subjects were positioned supine at rest and instructed not to breathe during image acquisition. Scan parameters were as follows: repetition time, 44 milliseconds, echo time, 9.6 to 9.9 milliseconds; flip angle, 25°; slice thickness, 3.4 to 4.2 mm (depending on the anatomy of the subject); square field of view, 34 × 34 cm to 40 × 40 cm; matrix dimensions, 512 × 192 pixels; and through-plane velocity encoding gradient, 150 cm/s.

The area ratio was calculated as the ratio of the area of the infrarenal aorta over the combined area of the left and right iliac arteries for each subject. Each area was computed from the image segments. The area of the left and right iliac arteries was an averaged value over all available segmented slices between the aortic and iliac bifurcations. Aortoiliac image segments were also processed to calculate average and maximum diameters. The oscillatory flow index (OFI) was calculated for each infrarenal waveform to compare retrograde flow in the abdominal aorta.¹⁴ OFI was calculated as

$$\text{OFI} = \frac{1}{2} \left(1 - \frac{\int_0^T Q dt}{\int_0^T |Q| dt} \right),$$

where Q is the flow rate and T is the period of each cardiac cycle. The OFI varies between 0 and 0.5, with an OFI value of 0 corresponding to a unidirectional flow throughout the cardiac cycle and a value of 0.5 corresponding to an oscillatory flow with a zero mean flow rate.

Generating subject-specific computer models. Subject-specific computer models were constructed with custom image-based modeling software by using techniques previously described.¹⁵ Briefly, path lines extracted from the MRA data were used to position two-dimensional slice planes normal to the vessel path. Luminal contour curves were obtained for these slice planes by using the level set method and lofted to create nonuniform rational B-spline surfaces and geometric solid models. One-dimensional models were generated from the three-dimensional models according to the path lines and the areas of the image segments. An automatic finite element mesh generator, Meshsim (Simmetrix, Inc, Clifton Park, NY), was used to discretize the models for the three-dimensional blood flow simulations and subsequent quantification of WSS. The finite element meshes had between 649,610 and 1,315,253 linear tetrahedral elements.

One-dimensional simulations. The nonlinear one-dimensional partial differential equations governing blood flow in deformable elastic vessels are derived from the equations of conservation of mass, balance of momentum, and a constitutive equation describing the material behavior of the vessel walls.^{16,17} Because analytic solutions to these equations cannot be obtained, a finite element method was used to obtain approximate numeric solutions for pressure and flow waveforms.¹⁸ The flow waveform at the level of the supraceliac aorta, acquired from PC-MRI, was applied as an inlet boundary condition, and impedance spectra were prescribed at the exits of the numerical domain as outlet boundary conditions.¹⁷ The impedance spectrum for each outlet was generated by using Womersley's elastic tube theory and an asymmetric binary fractal tree model of the distal vessels. By using vascular branching laws, a fractal tree model from a vessel of the size of the outlet branch to the size of capillary vessels was attained.¹⁹⁻²¹ Tree parameters were set to ensure that the resultant infrarenal flow rate matched measured data and that the outlet pressure matched the subject's measured mean cuff blood pressure. Simulations were run with an element size of 0.05 cm and 500 time steps over a cardiac cycle for at least 4 cycles until periodic solutions were obtained. To compare the pressure waveforms between SCI and control subjects, a decay time constant (τ) was calculated for each subject by fitting an exponential function of the form $e^{-t/\tau}$ to the pressure waveform in diastole. Large values of τ are characteristic of a slow diastolic pressure decay.

Three-dimensional simulations. To obtain infrarenal WSS, the incompressible Navier-Stokes equations were solved for blood velocity and pressure in rigid vessels by using a stabilized finite element method.²² The simulations were conducted with an approximate maximum element size of 0.09 cm and a time step of 0.0005 to 0.001 seconds for at least three cycles until the solution became periodic. The supraceliac flow waveform obtained from PC-MRI data for each subject was used as an inlet boundary condition, and resistance was specified at each outlet.²³ For three-dimensional analyses, outlet resistance for each branch vessel was computed by using a measured mean cuff pressure and infrarenal flow rate, together with literature data,²⁴ to assign relative flow between the celiac, mesenteric, renal, and iliac arteries. Simulations were performed by using this approach for resting conditions. To calculate a daily averaged WSS, 2 hours of light exercise shear stress were combined with 22 hours of resting shear stress for relatively sedentary but ambulatory control subjects.^{25,26} The light exercise condition was simulated by increasing the supraceliac flow rate by threefold and decreasing distal vessel resistances to attain a sixfold increase in iliac artery flow without causing a significant change in supraceliac blood pressure.²⁷ For nonambulatory SCI subjects, resting shear stress was used as the daily averaged WSS. We quantified the daily averaged WSS from the infrarenal to suprabi-furcational aorta to compare mean infrarenal WSS values between SCI and control subjects.

RESULTS

Subject characteristics. SCI and control subjects were well matched for age, height, and heart rate (Table I). Of the morphometric variables potentially relevant to AAA pathogenesis, SCI subjects demonstrated reduced body mass index; systolic, diastolic, and mean blood pressure; and prevalence of hypertension. The cohorts were well matched for smoking prevalence and intensity: 73% of the SCI group reported smoking an average 27.7 pack-years, whereas 62% of control subjects smoked an average 28.4 pack-years. However, 34% of the control group were current smokers, compared with 22% of the SCI cohort. Although SCI subjects had more chronic lower extremity wounds, the prevalence of major lower extremity amputation (below-knee or higher), partial foot amputation, or major abdominal trauma necessitating surgery was equal between groups (not significant).

In the SCI group, the length of time since injury (and subsequent profound lower extremity immobility) averaged 26 ± 13 years (mean \pm SD). Spinal injury occurred generally at or above the T12 vertebral level. Most spinal injuries resulted from traumatic events, including airplane, motor vehicle, motorcycle, and bicycle accidents; falls and diving accidents; and gunshot wounds and other combat injuries. Nontraumatic causes of spinal injury included multiple sclerosis, amyotrophic lateral sclerosis, Pott's disease, arachnoid cyst, epidural abscess, and arteriovenous malformations (Table II).

Table I. Patient characteristics

Variable	SCI subjects (n = 123)	Control subjects (n = 129)	P value
Age (y)	62.6 (9.5)	63.3 (8.8)	NS
Weight (pounds)	185.3 (35.1)	196.8 (40.5)	.02
Height (inches)	70.7 (3.0)	69.6 (2.9)	<.01
Body mass index (kg/m ²)	26.1 (4.6)	28.5 (5.1)	<.01
Systolic blood pressure (mm Hg)	125.5 (19.4)	137.4 (16.6)	<.01
Diastolic blood pressure (mm Hg)	71.6 (12.1)	81.2 (8.8)	<.01
Mean arterial pressure (mm Hg)	88.0 (17.4)	100.0 (9.8)	<.01
Heart rate (/min)	71.7 (12.7)	70.0 (11.9)	NS
Cholesterol (mg/dL)	179.1 (32.9)	191.0 (43.8)	.02
Family history of AAA disease	3 (2%)	12 (9%)	.03
Prior cardiovascular procedure	13 (11%)	31 (24%)	.01
Nonhealing lower extremity wounds	44 (36%)	13 (10%)	<.01
Amputation (major lower extremity)	3 (2%)	3 (2%)	NS
Amputation (partial foot)	6 (5%)	4 (3%)	NS
Abdominal trauma	7 (6%)	5 (4%)	NS
Diabetes mellitus	18 (15%)	24 (19%)	NS
Years of diabetic treatment	6.03 (7)	6.74 (6)	NS
Hypertension	46 (37%)	78 (60%)	<.01
Prior abdominal imaging	73 (59%)	41 (32%)	<.01
Smoking (ever)	93 (73%)	80 (62%)	NS
Smoking (current)	26 (21%)	45 (35%)	.02
Pack-years	29.2 (30.5)	28.4 (31.0)	NS

SCI, Spinal cord injury; NS, not significant; AAA, abdominal aortic aneurysm. Values are mean (SD) or n (%).

Table II. Locations and causes of spinal injury among the spinal cord injury cohort

Variable	No. subjects	%
Level of injury		
Cervical	51	43%
Cervicothoracic	1	1%
Thoracic	61	52%
Thoracolumbar	3	3%
Lumbar	2	2%
Cause of injury		
Traumatic	95	79%
Medical	15	21%

Aortic and iliac artery diameter. The average aortic diameter was larger in SCI than in control subjects (Table III). Aortic diameters 2.5 cm or more, considered enlarged but not aneurysmal, were also more prevalent in SCI subjects ($P < .01$), as were AAAs (aortic diameter ≥ 3.0 cm; $P < .05$). Iliac arteries were not visible in all subjects; measurements were obtained for 168 SCI iliac arteries and 227 control iliac arteries. No significant differences were noted between average iliac artery diameter or aneurysm prevalence; however, there were many more very small iliac arteries (<1.0 cm) in SCI subjects ($P < .0001$). When grouped by 0.2-cm increments, aortic diameters in SCI subjects tended to be higher than controls, whereas iliac arteries were smaller (Fig 1). Overall, there were significantly more AAAs, enlarged aortas, and very small iliac arteries in SCI subjects. A total of 20 aneurysms were found in 16 SCI subjects; 3 iliac aneurysms were found in subjects who also had an AAA.

Table III. Arterial diameter as a function of SCI status

Vascular status	SCI	Control	P value
n	123	129	
Aortic diameter (cm \pm SD)	2.3 (0.9)	2.0 (0.4)	<.01
Aorta ≥ 3.0 cm (AAA)	11 (8.9%)	4 (3.1%)	.04
Aorta ≥ 2.5 cm (AAA + enlarged)	31 (25.2%)	15 (11.6%)	<.01
n	168	227	
Iliac diameter (cm)	1.1 (0.3)	1.1 (0.2)	NS
Iliac ≥ 1.5 cm (aneurysm)	9 (5.4%)	12 (5.3%)	NS
Iliac ≥ 1.25 cm (aneurysm + enlarged)	26 (15.5%)	44 (19.4%)	NS
Iliac <1.0 cm	80 (47.6%)	59 (26.0%)	<.01

SCI, Spinal cord injury; AAA, abdominal aortic aneurysm; NS, not significant.

Values are mean (SD) or n (%).

Magnetic resonance arteriography. MRA of the abdominal aorta in all SCI subjects revealed a distinctive, consistent vascular phenotype of chronic SCI: irregular and ectatic distal aortic segments adjacent to markedly diminished iliac arteries. In contrast, control subjects displayed smoothly tapering aortas with comparatively wider-caliber iliac vessels and uniformly smooth walls (Fig 2). One SCI subject's aortic morphology (SCI 5) deviated markedly from the other four; further investigation confirmed that this subject had retained partial ambulatory status after his injury through the period of the study, so he was excluded from additional analysis. The mean diameter of the infrarenal aorta was 1.63 cm for SCI subjects and 1.54 cm for control subjects (not significant). However, the mean cross-sectional area ratio for aortas vs iliac arteries was 4.4 in

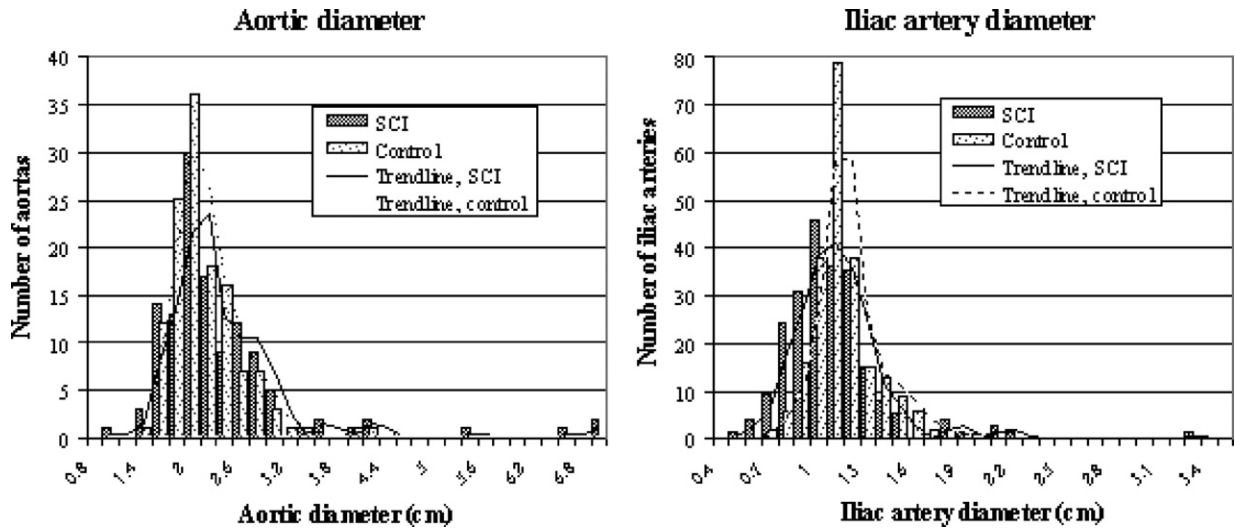


Fig 1. Distribution of aortic and iliac artery diameters with trend lines, spinal cord injury (SCI) vs control.

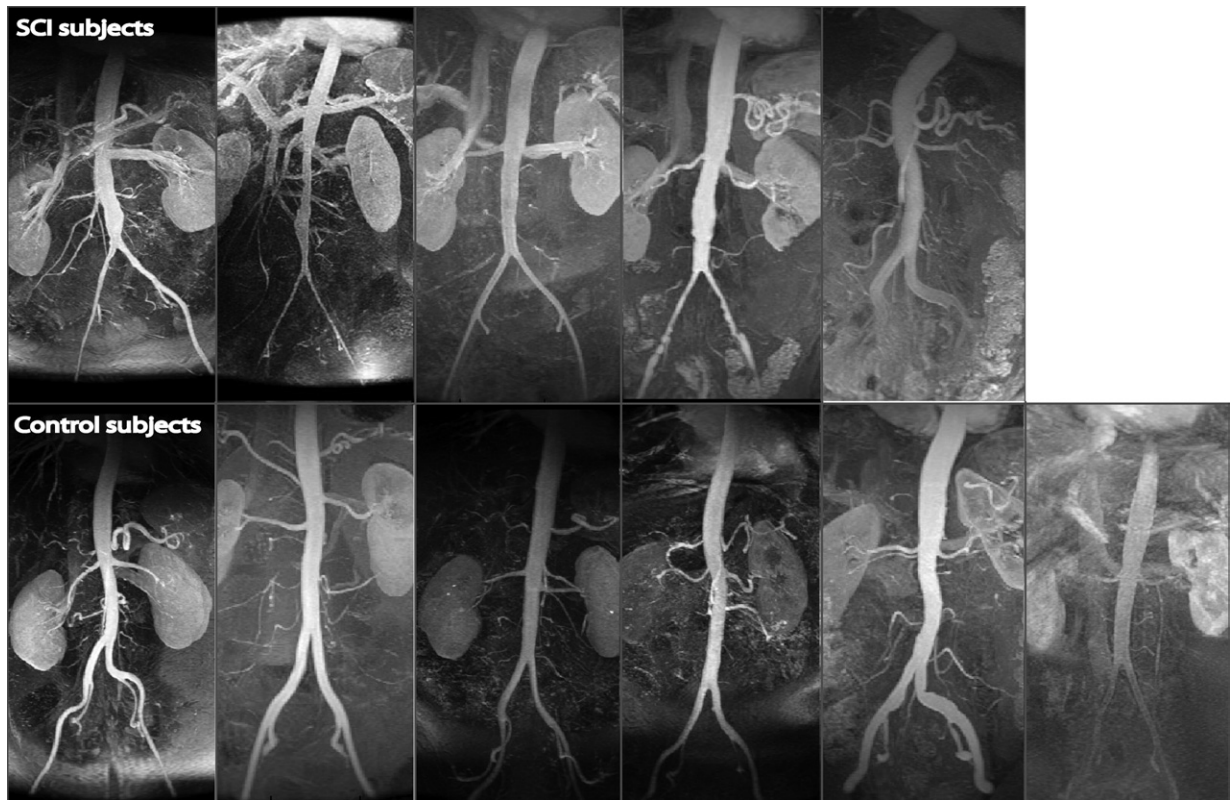


Fig 2. Magnetic resonance angiography of the abdominal aorta, spinal cord injury (SCI) vs control. Adapted from Tedesco et al., Future Cardiology 2006;2(4):478 with permission from Future Medicine Ltd.

SCI and 1.7 in control subjects ($P < .01$), thus demonstrating that the greater area ratio present in SCI subjects was due principally to relatively reduced iliac artery diameters.

Aortoiliac segments were compared for average diameters (Table IV, online only). The mean aortic diam-

eter (suprarenal aorta to bifurcation) for SCI subjects was 1.87 cm, compared with 1.87 cm for control subjects (not significant). However, as evident on MRA (Fig 2), SCI subjects exhibited focal aortic enlargement and increased variation in diameter along the length of the

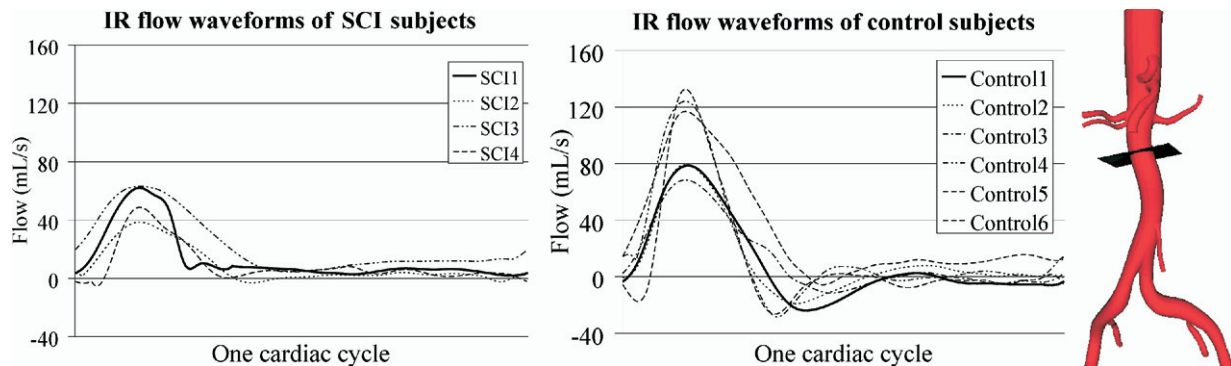


Fig 3. Infrarenal (IR) flow waveforms, spinal cord injury (SCI) vs control. Phase-contrast magnetic resonance imaging data were acquired for each subject at an IR slice plane perpendicular to the aorta and processed to compare the flow waveform over one cardiac cycle.

aorta. SCI subjects had smaller iliac arteries, with mean diameter of 0.70 cm, vs 0.91 cm for the control group ($P = .01$).

PC-MRI volumetric data were compared between the supraceliac and infrarenal aortic segments in the resting supine position. There was little difference between groups in the mean aortic flow rate. SCI subjects displayed mean supraceliac and infrarenal flow rates of 51.51 and 13.87 mL/s respectively, whereas control subjects averaged 52.30 and 13.70 mL/s. However, the infrarenal flow waveform was markedly different between groups. Control subjects showed triphasic flow waveforms with retrograde flow in diastole. SCI subjects mainly displayed biphasic more distributed flow with smaller peak values (Fig 3). Average OFI values were 0.006 for SCI subjects and 0.173 for control subjects ($P < .01$), thus signifying less oscillatory flow in nonambulatory SCI subjects.

One-dimensional flow and pressure analyses. The one-dimensional equations of blood flow were solved for pressure and flow waveforms (Fig 4). Flow waveforms for each subject varied significantly according to the impedance boundary conditions prescribed at the outlet vessels. Pressure waveforms lagged behind flow waveforms, as expected for pulsatile flow in elastic vessels. Wave morphology was influenced by the suprabi-furcation wave reflection and pressure decay.

Infrarenal flow waveforms calculated from the one-dimensional simulation were similar to the PC-MRI results (Fig 5). SCI infrarenal flow waveforms displayed distributed and little retrograde or oscillatory flow with a smaller peak value. The calculated mean OFI values were 0.032 for SCI subjects and 0.148 for control subjects ($P < .01$).

Pressure waveforms were similar for all outlet vessels, although pulse pressures increased slightly as the pressure waves propagated toward stiffened lower extremity vessels. The infrarenal pressure waveform was similar to the inlet pressure waveform, without noteworthy wave reflections from downstream vessels (Fig 5). However, SCI pressure waveforms showed slower decay in diastole in comparison with control waveforms. The average decay time constant

was 1.21 seconds for SCI subjects, vs 0.71 seconds for control subjects ($P < .01$; online supplement).

Three-dimensional flow and pressure analyses. Daily averaged WSS was computed for each model by solving the Navier-Stokes equations of blood flow (Fig 6). Daily averaged WSS in the SCI abdominal aorta was lower compared with the control aorta with 2 hours of simulated light exercise. Average values were 3.01 dyne/cm² for SCI vs 7.23 dyne/cm² for control subjects ($P = .06$). Control subjects varied widely in average aortic WSS, resulting in a nonsignificant P value. All SCI subjects consistently showed low mean aortic WSS.

DISCUSSION

This investigation documented characteristic morphologic and functional aortoiliac adaptations present in chronically nonambulatory patients after SCI. Although it is impossible to confirm the sole or primary cause of these adaptations in the absence of longitudinal observational data, the relative influence of the SCI alone vs the loss of ambulation secondary to SCI on aortic morphology was suggested by SCI subject 5, who retained limited walking ability and relatively normal aortic morphology. Little difference was noted in resting flow volume between groups, but aortic flow patterns were markedly abnormal in SCI subjects, characterized by reduced retrograde flow in diastole, a reduced OFI, slower diastolic pressure decay, and reduced WSS throughout the cardiac cycle.

There are approximately 250,000 persons with SCI in the United States, with 10,000 new injuries each year. In the mid-20th century, 80% of SCI patients died within 3 years of injury.²⁸ Recent innovations in SCI care focus on management of long-term complications, dramatically improving life expectancy. Neoplastic, cardiovascular, and accidental deaths are now replacing renal failure and urinary tract complications as the most common causes for mortality after SCI.²⁹ With improved longevity, coronary artery disease and stroke have replaced renal and pulmonary complications as the primary causes of cardiovascular morbidity.¹³ Among SCI patients surviving for more than 30 years

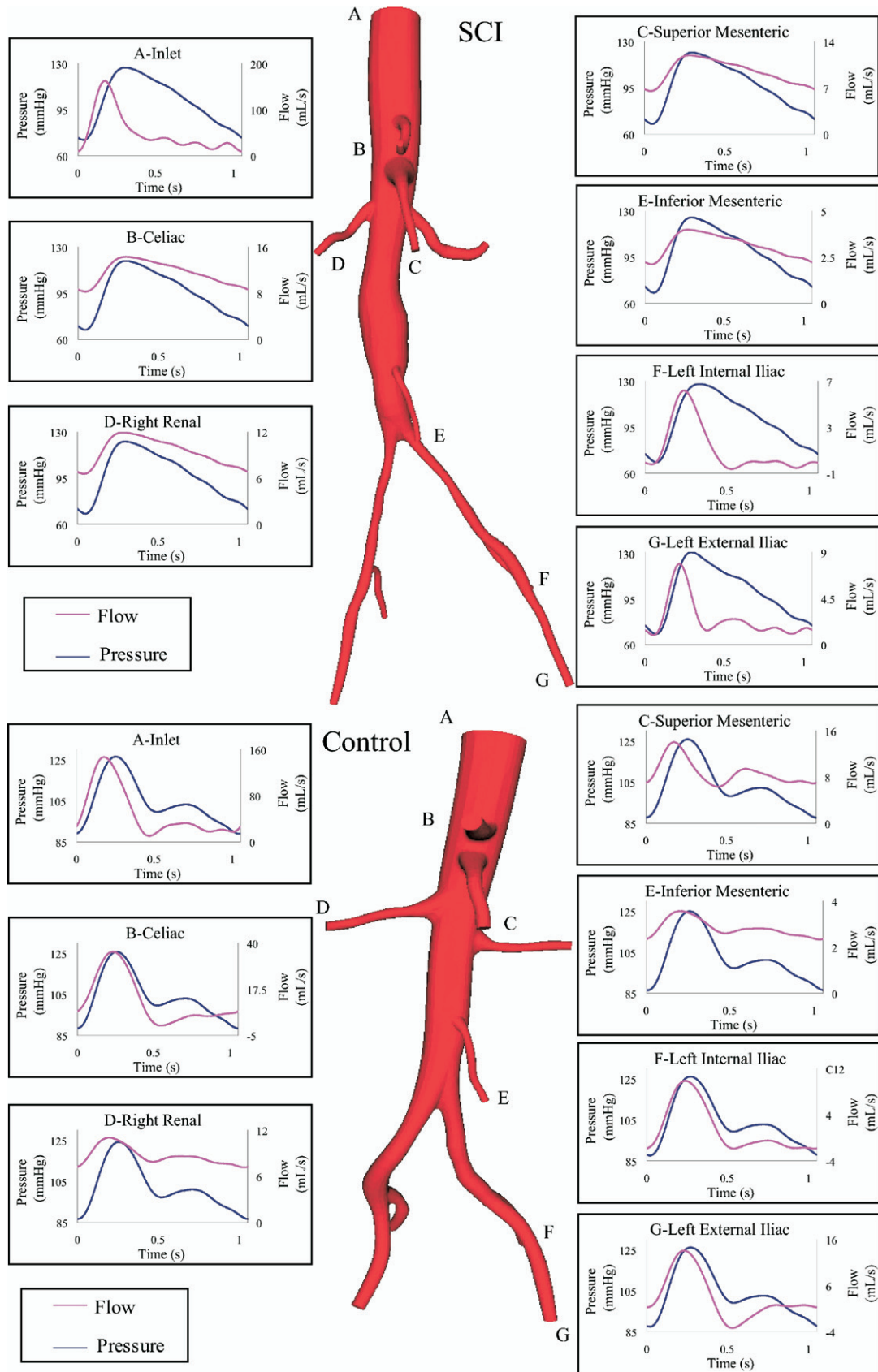


Fig 4. Pressure and flow waveforms from representative spinal cord injury (SCI) (top) and control (bottom) subjects.

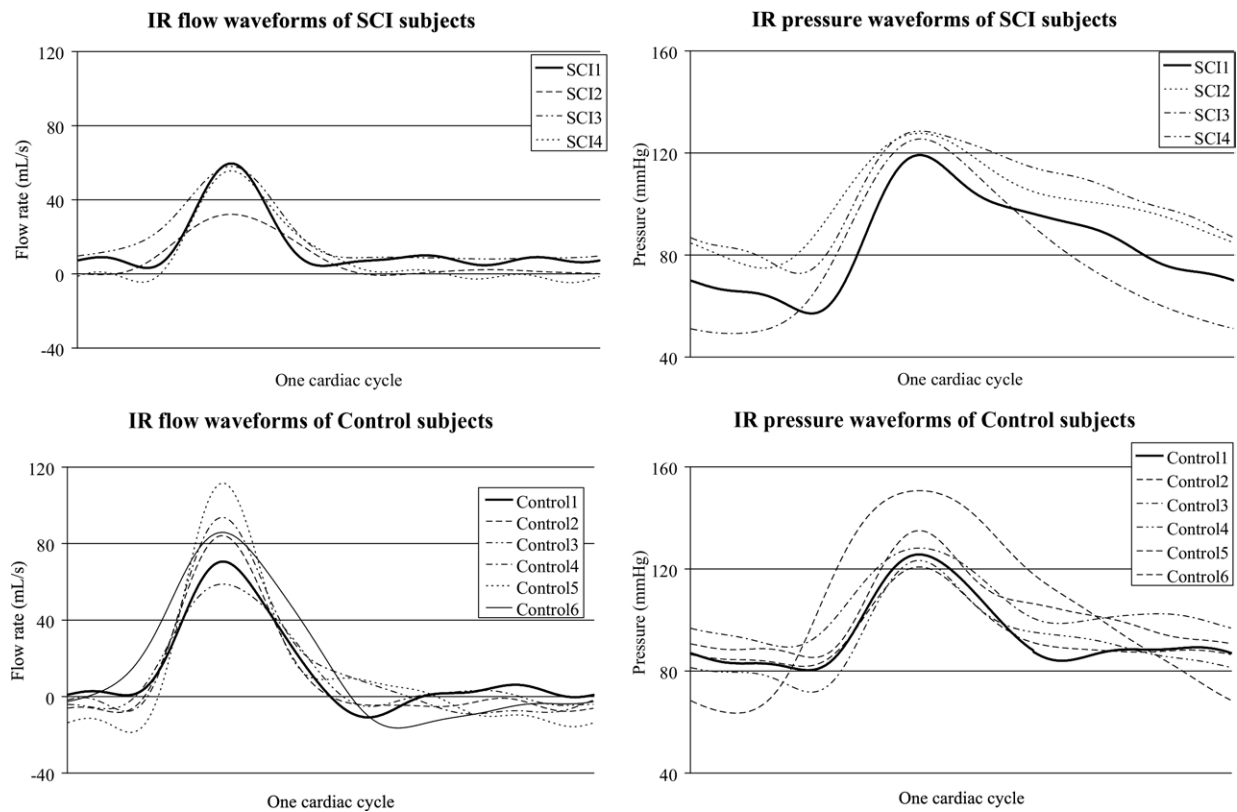


Fig 5. Infrarenal (*IR*) flow and pressure waveforms, spinal cord injury (*SCI*) vs control. Flow and pressure waveforms at the level of the infrarenal aorta were calculated from one-dimensional simulations.

after injury, 46% die of coronary heart disease,¹² a significantly higher percentage than that of age-matched and cardiovascular risk factor-matched ambulatory patients (35%).³⁰ Long-term inactivity is a well-recognized vascular risk factor, leading to loss of lean muscle mass, impaired glucose tolerance, hyperinsulinemia, and obesity. Diabetes is three times more common in SCI patients than in the general population,¹⁰ and lipid profiles are markedly unfavorable: high density lipoprotein levels are lower in SCI patients and vary inversely with injury level, whereas serum triglycerides are increased.¹¹ Considering the increased cardiovascular risk factors and incidence of cardiovascular death among this population, a finding of increased average aortic diameter is particularly significant in light of the known correlation between infrarenal aortic diameter and all-cause mortality.³¹

Although overall cardiovascular disease risk is increased in these patients, the unique hemodynamic environment of the infrarenal aorta after SCI (permanently sedentary state) may be a particularly significant risk factor for AAA disease. Luminal diameter varies as a function of WSS in both healthy and diseased arteries; arteries enlarge in response to increased flow, whereas decreased flow reduces artery diameter.³² Chronic exposure to laminar WSS of at least 5 to 10 dyne/cm² upregulates the expression of antithrombotic, antiproliferative, antiadhesive, and anti-inflammatory en-

dothelial molecular mediators and promotes endothelial cellularity and realignment.³³⁻³⁶ Oscillatory, stagnant, or complex flow vortices with low mean WSS zones occur at branch points and bifurcations and colocalize with high-probability areas for atherosclerotic lesions.^{37,38} The co-occurrence of diminutive iliac arteries and an enlarged infrarenal aorta, presumably due to reduced lower extremity activity and a complete absence of postexercise hyperemia in our SCI subjects, is not consistent with any known flow/remodeling relationship elsewhere in the human vasculature. An increased prevalence of AAA disease in peripheral arterial occlusive disease patients has been reported and may reflect altered aortic hemodynamic conditions secondary to distal vessel narrowing.^{39,40} Direct evidence of hemodynamic influences on AAA disease is available from biologically valid rodent models: creation of femoral arteriovenous fistulas reduces aneurysmal diameter and inflammation, whereas unilateral iliac artery ligation reduces aortic flow, increases aortic mural inflammation, and promotes AAA progression.³¹

To ensure that aortic remodeling processes related to inactivity were well under way in all subjects, a minimum 5-year period after SCI was required for study participation.⁴¹ The extended duration of SCI was also reassuring in that none of the AAAs identified was likely present before injury, nor was trauma an inciting factor. All AAAs were

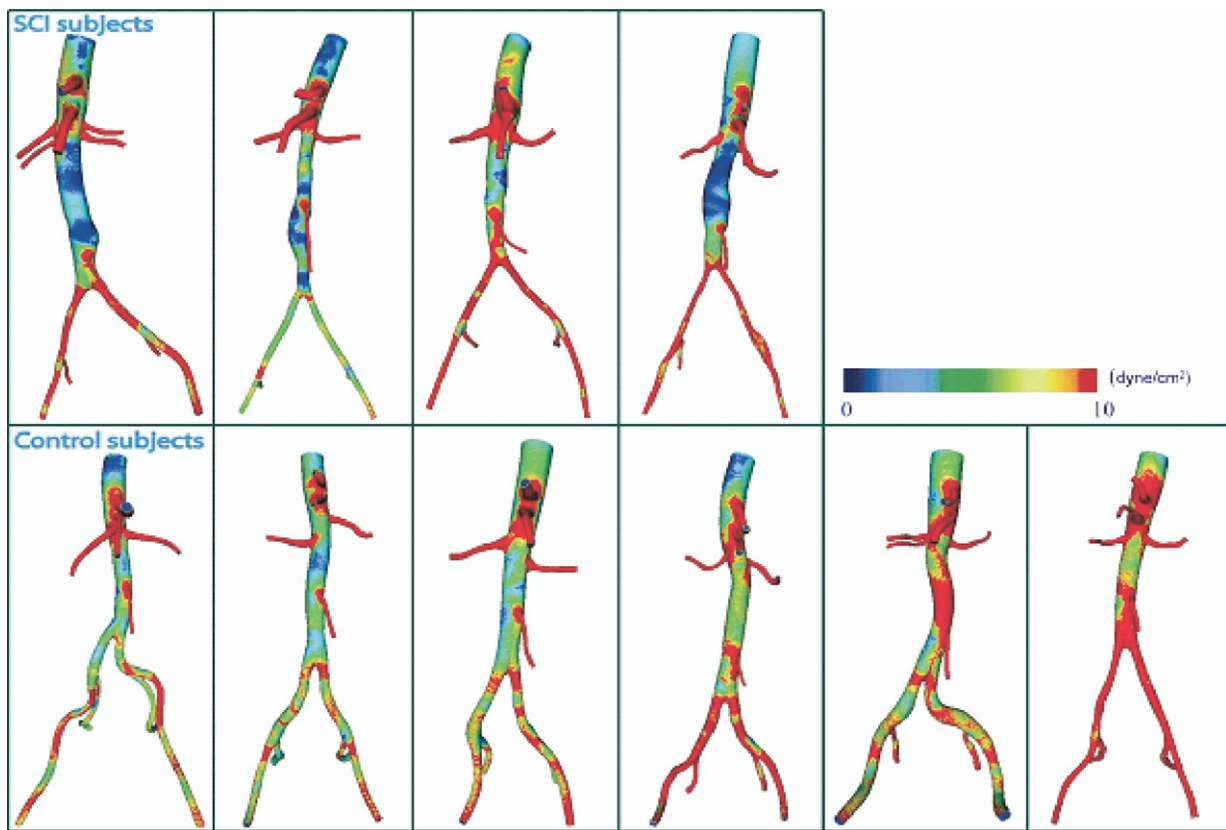


Fig 6. Daily averaged wall shear stress in computationally generated models of the abdominal aorta, spinal cord injury (SCI) vs control.

fusiform rather than saccular, and no chronic dissections were identified. Also, the level of SCI was typically well above the level of the infrarenal aorta. Although 60% of SCI subjects reported previous abdominal imaging scans (vs 31.8% of control subjects), new AAAs were still identified in 9% of participants. This seeming discrepancy was likely because annual renal ultrasound studies obtained on these patients are generally limited to the kidneys and urinary collecting system. Patients with known aneurysms were excluded from the study, so AAA prevalence in SCI patients may be even higher than our data would suggest.

Although a correlation between time after injury and aortic diameter or AAA prevalence would have provided additional reassurance regarding the underlying mechanism for aortic enlargement in SCI, no such relationship was present (data not shown). Given the number of patients imaged and the relatively tight distribution of aortic diameters present within the SCI cohort, however, this analysis is highly likely to underestimate such a correlation. Also, given the well-recognized relationship between age and AAA risk, the variable age of subjects at the time of SCI would confound potential correlations between duration of injury and aortic diameter. Aortic diameter enlargement may well progress at different rates in patients with SCI in their fifth decade as compared with their second.

Most demographic, physiologic, and morphometric differences between groups in this study were attributable to the consequences of SCI. Hypertension is a known risk factor for AAA, with an odds ratio (OR) of 1.23 in a prior veterans screening study,³ but systolic, diastolic, and mean arterial pressure or a history of hypertension necessitating medical treatment were all lower or less frequent in SCI subjects. Family history also increases AAA disease risk³ (OR = 1.95); this was more common among control subjects, likely because of a selection bias present in subjects choosing participation. Weight and body mass index, not previously recognized as independent AAA disease risk factors,⁴² were lower in SCI subjects, likely because of reduced muscle mass after injury. Cigarette smoking is the strongest recognized AAA risk factor in male veteran patients, with an OR of 5.57.⁴² The smoking prevalence in each cohort was comparable to those reported in the SCI veteran and general veteran patient population at large (76.8% and 74.2%, respectively). Current smokers are 1.5 times more likely than former smokers to have an AAA, and after smoking cessation, the risk decreases but does not return to baseline.^{3,43,44} More control than SCI subjects reported being current smokers (34.9% vs 21.1%; $P = .02$). Among the larger veteran patient population, 33.9% are current smokers.⁴⁴ The lower prevalence of smoking among our SCI cohort may have been due to better medical care, more

hospital admissions, or impaired upper extremity function. Regardless of the reasons for or effect of social and demographic differences between the groups, however, it is clear that a disproportionate risk related to hypertension, family, or cigarette-smoking history does not explain the excess number of AAAs identified in SCI subjects.

The prevalence of traditional AAA risk factors in our control group was similar to that described in the much larger Aneurysm Detection and Management (ADAM) trial.³ Although AAAs were less prevalent in our controls than in the ADAM veteran cohort (4.6%), given our comparatively modest sample size it is unlikely that any significant conclusion can be drawn from this discrepancy. We created our control group to provide concurrent comparisons between two patient populations within the same medical center. Given more observations, it is likely that the prevalence of AAA in both the SCI and controls groups may have been higher than was reported in this study.

Iliac artery ultrasound imaging in SCI subjects is limited by several technical factors, including a higher relative proportion of truncal adipose tissue. These challenges were evidenced by our ability to image only 68% of iliac arteries in SCI patients vs 88% in the control group. Although ultrasonography did not distinguish differences in average iliac artery diameter between groups, there were significantly more very small iliac arteries in the SCI group, and trend line analyses supported similar conclusions. The improved resolution capabilities of MRA clearly demonstrated the reduced iliac artery diameter characteristic of chronically nonambulatory SCI patients (Fig 2). The average iliac diameter calculations may have been biased by the relative difficulty in imaging smaller iliac arteries with ultrasonography, thus biasing the calculated means toward larger numbers.

Serum markers of inflammation are also correlated with AAA diameter and disease risk.^{45,46} Because of the nature of SCI, it is unlikely that such measurements would have been useful in differentiating AAA risk between cohorts in this study. Chronic SCI alone has been reported to increase C-reactive protein levels in otherwise healthy individuals,⁴⁵ and our SCI cohort experienced more chronic skin lesions, which also increase C-reactive protein. Although this was not quantified in this study, the SCI patients almost certainly had increased underlying inflammatory tone. Further investigation will be necessary to isolate the relative contributions of chronic inflammation and sedentary hemodynamic conditions to increased AAA risk in SCI subjects.

Because of the ability of MRA to define aortic geometry during the acquisition of blood velocity data via cine PC-MRI sequences, magnetic resonance provides simultaneous analysis of arterial structure and function. Subject-specific anatomic and flow data provide the basis for computational analysis of detailed spatial and temporal variations in velocity, pressure, and shear stress.¹⁷ SCI subjects demonstrated reduced retrograde flow in the infrarenal aorta. Infrarenal aortic flow waveforms were biphasic, as has been observed in patients with occlusive iliac disease,⁴⁷ although no focal iliac occlusive lesions were noted in MRA images of SCI subjects. The pressure de-

crease from the peak systolic value to end-diastolic levels also occurred much more slowly in SCI subjects, as measured with the diastolic pressure decay time constant, τ . By using a simple Windkessel lumped parameter analog model, the slower decay could be explained by a high downstream resistance, high capacitance, or both. The low diastolic flow and minimal flow reversal in the infrarenal aorta observed for SCI subjects confirms that the aorta and iliac and femoral arteries of SCI patients have low capacitance, thus making the slow pressure decay attributable to high downstream resistance. This slow pressure decay may precipitate the changes in the arterial wall that are characteristic of AAA. Although systolic blood pressures were not significantly higher in SCI vs control subjects, the SCI aorta experienced higher pressures for longer times because of a slower diastolic pressure decay. Collagen fibers are recruited in response to repetitive pressure-related transmural stress, and a longer load-bearing time may stimulate elastin degradation, collagen recruitment, and extracellular matrix remodeling, all histologic features of AAA development.^{48,49}

Aortic flow volume was equivalent between cohorts, as would be expected in resting subjects with intact lower extremities. On a time-averaged basis, however, significant flow differences exist between ambulatory controls and nonambulatory SCI subjects. Considering that modest lower extremity exercise in older individuals increases resting aortic WSS approximately 16-fold⁵⁰ and that even sedentary, obese individuals walk on average 80 min/d or 2 km at 5 km/h in "displacement activities,"²⁶ even minimally active individuals generate at least twice the total time-averaged WSS experienced by immobile SCI patients during a 24-hour period. It is not known how changing WSS throughout the day affects the endothelium. However, evidence is accumulating that repeated episodes of short periods of exercise (and related increases in arterial WSS) produce sustained cardiovascular benefits that may lower the risk for or progression of AAA disease. Short daily episodes are associated with marked reductions in all-cause mortality and vascular-related complications in patients with cardiovascular disease, arterial remodeling, and vasculoprotective endothelial phenotypes.⁵¹⁻⁵³ Because of the nature of SCI, however, activity-induced differences in aortic flow and WSS were not considered in this study.

Additional limitations were inherent in the nature of the study design. Because of the limited number of SCI patients available at any given time, 5 years was required to complete enrollment and ultrasound imaging. During that period, we upgraded through several increasingly sophisticated ultrasound platforms. Difficulties in imaging iliac arteries in earlier studies may have been due to technical limitations inherent in contemporary imaging equipment. For the one-dimensional simulation, impedance was generated by using an asymmetric binary fractal tree with the same arterial branching law for all outlets regardless of the downstream tissue or organ. Although vascular branching patterns vary according to the organs supplied, precise standard measurements are not available for abdominal organs or the lower extremities. Thus, the impedance func-

tions derived from these data may only approximate the actual physiological state. We have previously demonstrated, however, that impedance boundary conditions yield more realistic pressure and flow waveforms than prescribed pressure or resistance boundary conditions described elsewhere.¹⁷ Additional mathematical approximations include the use of an elastic constitutive equation¹⁹ and the assumptions inherent in one-dimensional theory whereby only the axial flow velocity and an area-mean pressure are computed.

WSS was computed by using a finite element method to solve the three-dimensional Navier-Stokes equations in rigid models. Current efforts are focused on solving the three-dimensional equations of blood flow in deformable elastic domains. The number of tetrahedral elements for the three-dimensional simulation ranged from 649,610 to 1,315,253. We did not prove the independence of the shear stress with respect to the mesh size, and the finite element mesh may not have been refined enough to resolve finer flow features, such as recirculation. However, on the basis of our experience with similar examples and our experimental validation studies, we believe that the methods used were the most exhaustive and realistic of those available.^{54,55} Finally, flow in the infrarenal aorta may display nonnewtonian fluid characteristics during periods of low velocity, as occurs during diastole; however, we assumed newtonian flow for all simulations.

Longitudinal data after infrarenal flow alterations after initial SCI, atrophic morphologic changes in the iliac vessels, and subsequent aortic dilatation and AAA do not yet exist. Imaging and flow analysis of nonaneurysmal SCI patients or computational models of normal aortas and small-caliber iliac arteries may be pursued in the future.

SUMMARY

Today many SCI patients are surviving long enough to develop age-related diseases such as AAA. In a consecutive series, 9% of male veteran chronic SCI patients were found to have previously unrecognized AAAs. Resting aortic hemodynamic conditions, as determined by MRA and PC-MRI, were markedly abnormal in SCI patients, characterized by reduced retrograde flow in diastole, reduced oscillatory flow, slower pressure decay in diastole, and reduced WSS throughout the cardiac cycle. Actual time-averaged differences between ambulatory individuals and SCI patients, although not measured, were likely to be much greater given the profound influence of lower extremity ambulation on aortic WSS. Whether SCI-specific hemodynamic conditions are the primary influence for or a consequence of accelerated aortic remodeling and aneurysmal degeneration awaits further investigation. These findings, if confirmed in larger studies, provide justification for AAA screening for SCI patients. These findings also provide additional confirmation that lower extremity exercise is a significant deterrent to aortic disease and AAA formation. The precise value of exercise in preventing aortic degeneration should be determined by a scientifically valid trial of supervised exercise testing in patients at risk for AAA disease.³⁷

We are grateful for the assistance of John K. Karwowski, Anne Sawyer-Glover, Beverly Tang, Shawna Thunen, Braden Victor, and Wanda O'Kelly.

AUTHOR CONTRIBUTIONS

Conception and design: CAT, RLD

Analysis and interpretation: JJY, HJK, TAA, IEV-C, CAT, RLD

Data collection: JJY, HJK, TAA, MTD, KKY, IP, RJH

Writing the article: JJY, HJK, RLD

Critical revision of the article: JJY, HJK, IEV-C, CAT, RLD

Final approval of the article: RLD, CAT

Statistical analysis: JJY, HJK

Obtained funding: JJY, HJK, RLD, CAT

Overall responsibility: JJY, HJK, CAT, RLD

REFERENCES

- Norman PE, Jamrozik K, Lawrence-Brown MM, Le MT, Spencer CA, Tuohy RJ, et al. Population based randomised controlled trial on impact of screening on mortality from abdominal aortic aneurysm. *BMJ* 2004; 329:1259.
- Ashton HA, Buxton MJ, Day NE, Kim NG, Marteau TM, Scott RA, et al. The Multicentre Aneurysm Screening Study (MASS) into the effect of abdominal aortic aneurysm screening on mortality in men: a randomised controlled trial. *Lancet* 2002;360:1531-9.
- Lederle FA, Johnson GR, Wilson SE, Chute EP, Littooy FN, Bandyk D, et al. Prevalence and associations of abdominal aortic aneurysm detected through screening. Aneurysm Detection and Management (ADAM) Veterans Affairs Cooperative Study Group. *Ann Intern Med* 1997;126: 441-9.
- Taylor CA, Hughes TJ, Zarins CK. Effect of exercise on hemodynamic conditions in the abdominal aorta. *J Vasc Surg* 1999;29:1077-89.
- Vollmar JF, Paes E, Pauschinger P, Henze E, Friesch A. Aortic aneurysms as late sequelae of above-knee amputation. *Lancet* 1989; 2:834-5.
- McMillan WD, Pearce WH, Yao JS. Differential patterns of atherosclerotic disease in patients with unilateral hemiparesis resulting from poliomyelitis: case reports demonstrating the possible effect of hemodynamics. *Cardiovasc Surg* 1997;5:435-8.
- Gordon IL, Kohl CA, Arefi M, Complin RA, Vulpe M. Spinal cord injury increases the risk of abdominal aortic aneurysm [retraction 1997; 63:111]. *Am Surg* 1996;62:249-52.
- Sandgren T, Sonesson B, Ryden A, Lanne T. Arterial dimensions in the lower extremities of patients with abdominal aortic aneurysms—no indications of a generalized dilating diathesis. *J Vasc Surg* 2001;34: 1079-84.
- Bauman WA, Kahn NN, Grimm DR, Spungen SM. Risk factors for atherogenesis and cardiovascular autonomic function in persons with spinal cord injury. *Spinal Cord* 1999;37:601-16.
- Bauman WA, Spungen AM. Disorders of carbohydrate and lipid metabolism in veterans with paraplegia or quadriplegia: a model of premature aging. *Metabolism* 1994;43:749-56.
- Bauman WA, Spungen AM, Zhong YG, Rothstein JL, Petry C, Gordon SK. Depressed serum high density lipoprotein cholesterol levels in veterans with spinal cord injury. *Paraplegia* 1992;30:697-703.
- Whiteneck GG, Charlifue SW, Frankel HL, Fraser MH, Gardner BP, Gerhart KA, et al. Mortality, morbidity, and psychosocial outcomes of persons spinal cord injured more than 20 years ago. *Paraplegia* 1992; 30:617-30.
- Zeilig G, Dolev M, Weingarden H, Blumen N, Shemesh Y, Ohry A. Long-term morbidity and mortality after spinal cord injury: 50 years of follow-up. *Spinal Cord* 2000;38:563-6.
- Taylor CA, Cheng CP, Espinosa LA, Tang BT, Parker D, Herfkens RJ. In vivo quantification of blood flow and wall shear stress in the human

- abdominal aorta during lower limb exercise. *Ann Biomed Eng* 2002;30:402-8.
15. Wilson NM, Wang KC, Dutton RW, Taylor CA. A software framework for creating patient specific geometric models from medical imaging data for simulation based medical planning of vascular surgery. *Lecture Notes in Computer Science*; In: *Proceedings of the 4th Annual Conference on Medical Image Computing and Computer-Assisted Intervention*. Springer-Verlag, London, UK 2001. p. 449-56.
 16. Hughes TJR, Lubliner J. On the one-dimensional theory of blood flow in the larger vessels. *Math Biosci* 1973;18:161-70.
 17. Vignon I, Taylor CA. Outflow boundary conditions for one-dimensional finite element modeling of blood flow and pressure waves in arteries. *Wave Motion* 2004;39:361-74.
 18. Wan J, Steele B, Spicer SA, Strohsband S, Feijoo GR, Hughes TJ, et al. A one-dimensional finite element method for simulation-based medical planning for cardiovascular disease. *Comput Methods Biomech Biomed Eng* 2002;5:195-206.
 19. Steele BN, Olufsen M, Taylor CA. Fractal network model for simulating abdominal and lower extremity blood flow during resting and exercise conditions. Accepted for publication in *Comput Methods Biomech Biomed Eng*. 2006.
 20. Olufsen MS. Structured tree outflow condition for blood flow in larger systemic arteries. *Am J Physiol* 1999;276:H257-68.
 21. Womersley JR. Oscillatory motion of a viscous liquid in a thin-walled elastic tube. I. The linear approximation for long waves. *Philosophical Magazine* 1955;46(373):199-221.
 22. Taylor CA, Hughes TJ, Zarins CK. Finite element modeling of three-dimensional pulsatile flow in the abdominal aorta: relevance to atherosclerosis. *Ann Biomed Eng* 1998;26:975-87.
 23. Vignon-Clementel IE, Figueroa CA, Jansen KC, Taylor CA. Outflow boundary conditions for three-dimensional finite element modeling of blood flow and pressure in arteries. *Comput Methods Appl Mech Eng* 2006;195:3776-96.
 24. Ku DN, Glagov S, Moore JE Jr, Zarins CK. Flow patterns in the abdominal aorta under simulated postprandial and exercise conditions: an experimental study. *J Vasc Surg* 1989;9:309-16.
 25. Vogels N, Egger G, Plasqui G, Westerterp KR. Estimating changes in daily physical activity levels over time: implication for health interventions from a novel approach. *Int J Sports Med* 2004;25:607-10.
 26. Schutz Y, Weinsier S, Terrier P, Durrer D. A new accelerometric method to assess the daily walking practice. *Int J Obes Relat Metab Disord* 2002;26:111-8.
 27. Cheng CP, Herfkens RJ, Taylor CA. Abdominal aortic hemodynamic conditions in healthy subjects aged 50-70 at rest and during lower limb exercise: in vivo quantification using MRI. *Atherosclerosis* 2003;168:323-31.
 28. Guttman L. *Spinal cord injuries: comprehensive management and research*. Oxford: Blackwell Science Ltd; 1976.
 29. DeVivo MJ, Krause JS, Lammertse DP. Recent trends in mortality and causes of death among persons with spinal cord injury. *Arch Phys Med Rehabil* 1999;80:1411-9.
 30. *Morbidity and mortality: 2004 chartbook on cardiovascular, lung and blood diseases*. Thomas Thom, National Institutes of Health National Heart, Lung and Blood Institute, Bethesda, MD; 2004.
 31. Norman P, Le M, Pearce C, Jamrozik K. Infrarenal aortic diameter predicts all-cause mortality. *Arterioscler Thromb Vasc Biol* 2004;24:1278-82.
 32. Hoshina K, Sho E, Sho M, Nakahashi TK, Dalman RL. Wall shear stress and strain modulate experimental aneurysm cellularity. *J Vasc Surg* 2003;37:1067-74.
 33. Cybulsky MI, Gimbrone MA Jr. Endothelial expression of a mononuclear leukocyte adhesion molecule during atherogenesis. *Science* 1991; 251:788-91.
 34. Zarins CK, Bomberger RA, Glagov S. Local effects of stenoses: increased flow velocity inhibits atherogenesis. *Circulation* 1981;64(2 Pt 2):II221-7.
 35. Inoue N, Ramasamy S, Fukai T, Nerem RM, Harrison DG. Shear stress modulates expression of Cu/Zn superoxide dismutase in human aortic endothelial cells. *Circ Res* 1996;79:32-7.
 36. De Keulenaer GW, Chappell DC, Ishizaka N, Nerem RM, Alexander RW, Griendling KK. Oscillatory and steady laminar shear stress differentially affect human endothelial redox state: role of a superoxide-producing NADH oxidase. *Circ Res* 1998;82:1094-101.
 37. Cornhill JF, Herderick EE, Sary HC. Topography of human aortic sudanophilic lesions. *Monogr Atheroscler* 1990;15:13-9.
 38. Gimbrone MA Jr, Topper JN, Nagel T, Anderson KR, Garcia-Cardena G. Endothelial dysfunction, hemodynamic forces, and atherogenesis. *Ann N Y Acad Sci* 2000;902:230-9; discussion 239-40.
 39. Hassen-Khodja R, Le Bas P, Pittaluga P, Batt M, Declémy S, Bariseel H. Abdominal aortic aneurysm and lower-limb occlusive arterial disease. *J Cardiovasc Surg (Torino)* 1998;39:141-5.
 40. van den Bosch M, van der Graaf W, Eikelboom B, Algra A, Mali WP. SMART Study Group. Distal aortic diameter and peripheral arterial occlusive disease. *J Vasc Surg* 2001;34:1085-9.
 41. De Groot PC, Van Kuppevelt DH, Pons C, Snoek G, Van Der Woude LH, Hopman MT. Time course of arterial vascular adaptations to inactivity and paralysis in humans. *Med Sci Sports Exerc* 2003;35:1977-85.
 42. Lederle FA, Johnson GR, Wilson SE, Gordon IL, Chute EP, Littooy FN, et al. Relationship of age, gender, race, and body size to infrarenal aortic diameter. The Aneurysm Detection and Management (ADAM) Veterans Affairs Cooperative Study Investigators. *J Vasc Surg* 1997;26:595-601.
 43. Spungen AM, Lesser M, Almenoff PL, Bauman WA. Prevalence of cigarette smoking in a group of male veterans with chronic spinal cord injury. *Mil Med* 1995;160:308-11.
 44. Klevens RM, Giovino GA, Peddicord JP, Nelson DE, Mowery P, Grummer-Strawn L. The association between veteran status and cigarette-smoking behaviors. *Am J Prev Med* 1995;11:245-50.
 45. Frost F, Roach MJ, Kushner I, Schreiber P. Inflammatory C-reactive protein and cytokine levels in asymptomatic people with chronic spinal cord injury. *Arch Phys Med Rehabil* 2005;86:312-7.
 46. Vainas T, Lubbers T, Stassen FR, Hergreen SB, van Dieijen-Visser MP, Bruggeman CA, et al. Serum C-reactive protein level is associated with abdominal aortic aneurysm size and may be produced by aneurysmal tissue. *Circulation* 2003;107:1103-5.
 47. Suzuki E, Kashiwagi A, Nishio Y, Kojima H, Maegawa H, Haneda M, et al. Usefulness of waveform analysis of popliteal artery in type II diabetic patients using gated magnetic resonance 2D-cine-PC imaging and ³¹P spectroscopy. *Diabetologia* 2000;43:1031-8.
 48. Watton PN, Hill NA, Heil M. A mathematical model for the growth of the abdominal aortic aneurysm. *Biomech Model Mechanobiol* 2004;3:98-113.
 49. Wang YN, Sanders JE. How does skin adapt to repetitive mechanical stress to become load tolerant? *Med Hypotheses* 2003;61:29-35.
 50. Cheng CP, Herfkens RJ, Taylor CA. Comparison of abdominal aortic hemodynamics between men and women at rest and during lower limb exercise. *J Vasc Surg* 2003;37:118-23.
 51. Bassuk SS, Manson JE. Physical activity and the prevention of cardiovascular disease. *Curr Atheroscler Rep* 2003;5:299-307.
 52. Rehman J, Li J, Parvathaneni L, Karlsson G, Panchal VR, Temm CJ, et al. Exercise acutely increases circulating endothelial progenitor cells and monocyte-/macrophage-derived angiogenic cells. *J Am Coll Cardiol* 2004;43:2314-8.
 53. Liu Y, Lai Y, Nagaraj A, Kane B, Hamilton A, Greene R, et al. Pulsatile flow simulation in arterial vascular segments with intravascular ultrasound images. *Med Eng Phys* 2001;23:583-95.
 54. Ku JP, Elkins CJ, Taylor CA. Comparison of CFD and MRI flow and velocities in an in vitro large artery bypass graft model. *Ann Biomed Eng* 2005;33:257-69.
 55. Ku JP, Drancy MT, Arko FR, Lee WA, Chan FP, Pelc NJ, et al. In vivo validation of numerical prediction of blood flow in arterial bypass grafts. *Ann Biomed Eng* 2002;30:743-52.

Submitted May 15, 2006; accepted Aug 14, 2006.

Additional material for this article may be found online at www.jvascsurg.org.

Table IV, online only. Average and maximum aortic and iliac diameters by MRI in SCI and control subjects

<i>Subject</i>	<i>Average aortic diameter, suprarenal to bifurcation (cm ± SD)</i>	<i>Average infrarenal aortic diameter (cm ± SD)</i>	<i>Maximum infrarenal aortic diameter (cm)</i>	<i>Average iliac diameter (cm ± SD)</i>	<i>Maximum iliac diameter (cm)</i>
SCI 1	1.8 ± 0.2	1.7 ± 0.1	1.9	0.6 ± 0.2	1.2
SCI 2	1.6 ± 0.3	1.4 ± 0.2	1.5	0.5 ± 0.0	0.6
SCI 3	1.8 ± 0.3	1.5 ± 0.1	1.7	0.6 ± 0.0	0.7
SCI 4	2.0 ± 0.3	1.8 ± 0.3	2.2	0.5 ± 0.1	0.7
SCI 5	2.0 ± 0.3	1.8 ± 1.1	1.9	1.2 ± 0.1	1.3
SCI average	1.9	1.6	1.8	0.7	0.9
Control 1	1.7 ± 0.3	1.4 ± 0.0	1.4	0.8 ± 0.0	0.9
Control 2	1.8 ± 0.2	1.6 ± 0.1	1.7	1.0 ± 0.2	1.5
Control 3	1.9 ± 0.3	1.6 ± 0.1	1.7	0.8 ± 0.1	1.1
Control 4	1.8 ± 0.3	1.6 ± 0.1	1.7	0.9 ± 0.1	1.1
Control 5	2.0 ± 0.4	1.5 ± 0.1	1.6	1.2 ± 0.1	1.4
Control 6	1.9 ± 0.3	1.5 ± 0.3	1.5	0.7 ± 0.1	0.9
Control average	1.9	1.5	1.6	0.9	1.1